Gene corrections for two types of disease-related single nucleotide polymorphisms in patient-derived cells via CRISPR/Cas9 system

Do-Hun Kim

Department of Medical Science

The Graduate School, Yonsei University

Gene corrections for two types of disease-related single nucleotide polymorphisms in patient-derived cells via CRISPR/Cas9 system

Do-Hun Kim

Department of Medical Science

The Graduate School, Yonsei University

Gene corrections for two types of disease-related single nucleotide polymorphisms in patient-derived cells via CRISPR/Cas9 system

Directed by Professor Dong-Wook Kim

The Doctoral Dissertation
Submitted to the Department of Medical Science,
The Graduate School of Yonsei University
in partial fulfillment of the requirements for the degree of
Doctor of Philosophy

Do-Hun Kim

December 2020

This certifies that the Doctoral Dissertation of Do-Hun Kim is approved.

Thesis Supervisor:	Dong-Wook Kim
Thesis Committee Chair:	Myoung Hee Kim
Thesis Committee Member #1	Hyongbum (Henry) Kim
Thesis Committee Member #2	Kook In Park
Thesis Committee Member #3	Chuhl Joo Lyu

The Graduate School

Yonsei University

December 2020

Acknowledgements

First of all, I would like to express my deepest gratitude to my advisor, Prof. Dong-Wook Kim for his support and advice throughout the research. His counsel and guidance have always been a great help to me. I am also deeply grateful to Prof. Hyongbum (Henry) Kim and Dr. Chul-Yong Park for their advice and guidance which have made me a better scholar.

I would like to thank to all my laboratory colleagues who encouraged me to keep moving forward and stay confident during the demanding and rigorous life of a Ph.D. student.

Last but not least, I have to acknowledge and convey my sincere gratitude to my father, my mother, and my brother for their unconditional love and support.

Do-Hun Kim

Table of Contents

LIST OF FIGURES

LIST OF TABLES

Abstract

Gene corrections for two types of disease-related single nucleotide polymorphisms in patient-derived cells via CRISPR/Cas9 system

Do-Hun Kim

Department of medical Science

The Graduate School, Yonsei University

(Directed by Professor Dong-Wook Kim)

Target-specific gene modification using engineered nucleases such as zinc finger nuclease (ZFN), transcription activator-like effector nuclease (TALEN), and type II clustered regularly interspaced short palindromic repeats (CRISPR)/CRIPSR-associated protein 9 (Cas9), is a promising strategy to correct various human genetic disorders. Among these techniques, CRISPR/Cas9 can be applied most easily to the desired target site. The target specificity of CRISPR/Cas9 can be modified by simply replacing the guide RNA (gRNA), making it more suitable to deal with different types of mutations than other nucleases. Therefore, CRISPR/Cas9 has been researched as the most useful tool for treating mutations associated with human genetic diseases. There are more than 54,000 human

genetic variants associated with disease, and 58% of human genetic diseases are caused by single nucleotide polymorphisms (SNPs). Among these diseases, mitochondrial DNA (mtDNA)-related diseases and coagulation factor VII (FVII) deficiency are known as most the common diseases caused by SNPs. This study performed genetic modifications for these two types of diseases using CRISPR/Cas9. First, for mitochondrial gene editing, a mitochondria-specific Cas9 (mitoCas9) was constructed, which successfully migrated to mitochondria. However, when plasmids were delivered that encode mitoCas9 and gRNA for mitochondrial genome editing into patient-derived cells, the gRNA did not translocate to mitochondria properly. Therefore, CRISPR/Cas9 did not work as expected in mitochondria. On the other hand, when mitoCas9 and gRNA are delivered as a ribonucleoprotein (RNP) complex, which directly injects mitoCas9 and gRNA into the cytosol, some of the mutant mtDNA in patient-derived heteroplasmic cells could be removed. Thus the total amount of mtDNA could be downregulated by the mitoCas9/gRNA RNP complex. Although these changes were insufficient to enable functional recovery due to a low translocation efficiency and a short half-life of the RNP complex, these results suggest that mitoCas9/gRNA RNP complexes can be a useful method for mitochondrial genome editing. Next, for gene correction of FVII deficiency-related SNPs, FVII-induced pluripotent stem cells (FVII-iPSCs) were generated from patient-derived fibroblasts, which contain novel compound heterozygous mutations in the blood coagulation factor *FVII* locus. By using the CRISPR/Cas9 system and single-stranded oligodeoxynucleotides (ssODNs) as the donor template, the two mutations were

sequentially corrected. After differentiation of gene-corrected FVII-iPSCs to hepatocyte-like cells (HLCs), I confirmed that the FVII activity of the FVIIC-iPSC-derived HLCs was restored to a similar level as wild type cells. Based on these results, this was an efficient method for gene correction of various disease-related SNPs using a CRISPR/Cas9 system, and this technique could be a valuable tool for gene therapy and cell therapy of various SNP-related diseases.

Key words: mitochondria, iPSC, CRISPR/Cas9, Factor VII deficiency, gene correction

Gene corrections for two types of disease-related single nucleotide polymorphisms in patient-derived cells via CRISPR/Cas9 system

Do-Hun Kim

Department of medical Science

The Graduate School, Yonsei University

(Directed by Professor Dong-Wook Kim)

I. INTRODUCTION

Genome engineering methods, especially engineered nuclease such as zing-finger nuclease (ZFN), transcription activator-like effector nuclease (TALEN) and clustered regularly interspaced short palindromic repeats (CRISPR) and CRISPR-associated protein 9 (Cas9) system, have evolved dramatically over the past decades.[1] Among these engineered nucleases, CRISPR/Cas9 is the most recently developed engineering method. Unlike other nucleases, CRISPR/Cas9 consists of two separate components, guide RNA (gRNA) for target recognition and Cas9 for endonuclease. gRNA is about 100 bp in size and can be easily made synthetically. For this reason, it is easy to construct custom

endonuclease and repurposing it.[2,3] CRISPR/Cas9 is considered as a promising approach to correct pathogenic mutations in various human diseases.

There are more than 54,000 human genetic variants associated with disease. Among the various mutations such as insertion, deletion, and structural variant, the most common type of known pathogenic variants is a single-nucleotide polymorphism (SNP), which account for 58% of all disease-related mutations.[4-6] Efficient manipulation of pathogenic SNPs is important for study and development of gene therapy for SNP-related genetic disorders and CRISPR/Cas9 is most suitable than any other engineered nuclease to deal with them.

Mitochondria are membrane-bound cell organelles and found in all nucleated cells. Main role of mitochondria is generation of cellular ATP, which is more than 90% of total ATP generation.[7] Mitochondria contain their own genome, mitochondrial DNA (mtDNA). In human case, mtDNA is 16.6 kb size of circular DNA and encodes 37 genes for mitochondrial biogenesis, which includes 13 polypeptides for oxidative phosphorylation system (OXPHOS), rRNAs and tRNAs for their translation within the organelle (2 rRNAs and 22 tRNAs).[8] At least 250 SNPs in mtDNA have been known to be associated with diseases.[7] Single mitochondrion may contain up to 20 copies of mtDNA molecules and single cell may have hundreds of mitochondria.[9,10] Because there are multiple copies of mtDNA in a cell, sometimes it harbors a mixture of normal and mutated mtDNAs, which is called as heteroplasmy.[11] The level of heteroplasmy (i.e., the percentage of mutant mtDNA) is important to the expression of the disease phenotype. symptoms of the disease

appear when the ratio of mutant to wild-type mtDNA rises above a certain percentage.[12-14] So, regulation of mutant mtDNA is important for treatment of mitochondria-related disease. Recently, some studies have been reported to control mtDNA using engineered nucleases. ZFN and TALEN was able to successfully control mtDNA.[15-17] Although there are some reports that CRISPR/Cas9 can regulate mtDNA,[18,19] but there is still controversy about whether it is possible or not.[20]

Factor VII (FVII) deficiency is the most frequent among rare bleeding disorders. It is usually transmitted in an autosomal recessive manner with an incidence of one per 500,000 in the general population.[21] Clinical symptoms are heterogeneous and range from miscellaneous minor bleeding to severe life-threatening hemorrhages, such as cerebral, gastrointestinal, and joint hemorrhages.[22] Various types of mutations are responsible for FVII deficiency. Among them, the most common type of mutation is SNP (The FVII mutations database, http://www.umd.be/F7/W_F7/index.html). About 80% of all reported mutations are known as SNPs. In addition, FVII deficiency is often caused by compound mutations.[23] Therefore, it is necessary to establish an efficient SNP correction method for multiple SNP-related diseases such as FVII deficiency.

Because most of the mitochondrial disease-related and FVII deficiency related mutations are SNPs, gene correction by TALENs or ZFNs is quite laborious and time-consuming. It is more suitable to use CRISPR/Cas9 system for effectively dealing with these various SNPs. Therefore, in this study, I aimed to make gene correction using CRISPR/Cas9 in patient-derived cells carrying mitochondria or FVII mutations.

II. MATERIALS AND METHODS

1. Cell culture, electroporation & generation of iPSCs

K562 (ATCC, Manassas, Virginia, USA) cells were grown in RPMI-1640 (Thermo Fisher Scientific, Waltham, Massachusetts) with 10% FBS (Thermo Fisher Scientific) and a penicillin/streptomycin (Thermo Fisher Scientific). BJ (ATCC) fibroblasts were maintained in MEM (Thermo Fisher Scientific) supplemented with 10% FBS, 0.1 mM nonessential amino acids (NEAA, Thermo Fisher Scientific), and a penicillin/streptomycin. SH-SY5Y cells were maintained in DMEM (Thermo Fisher Scientific) supplemented with 15% FBS.

For generation of patient-derived iPSCs, episomal plasmids encoding reprogramming factors were used as reported.[24] In brief, patient-derived fibroblasts grown in DMEM (Thermo Fisher Scientific) supplemented with 10% FBS and 1% NEAA were electroporated using a microporator system (Neon, Thermo Fisher Scientific) with 3 μg of episomal plasmid mixtures. After three 10 milliseconds pulse with a voltage of 1,650, the cells were grown in DMEM containing 10% FBS and 1% NEAA. Seven days after transfection, cells were transferred onto a STO feeder layer. iPSC colonies like hESCs were picked up mechanically and further cultured for characterization. Undifferentiated patient-derived iPSCs were cultured on mouse STO fibroblasts (ATCC) under previously described growth condition.[25]

2. RNA extraction, cDNA synthesis, and qPCR

Total RNA was extracted using the Easy-Spin® Total RNA Extraction kit (iNtRON Biotechnology, Seongnam, Korea) according to the manufacturer's instructions. cDNA was synthesized from 1 μg of total RNA using PrimeScriptTM RT Master Mix (TAKARA Bio Inc., Otsu, Japan). qPCR was performed using FastFire qPCR PreMix (TIANGEN, Beijing, Chian) in a CFX96 Real-Time System (Bio-Rad, California, USA). The transcription level for each targeted gene was normalized to GAPDH expression. Primer sequences are listed in Table 2.

3. Genomic DNA extraction, genotyping PCR and ARMS qPCR

Total genomic DNA was extracted by DNeasy Blood & Tissue kit (Qiagen) as the manufacturer's manual. Total contents of mtDNA in patient-derived cells were measured by qPCR and heteroplasmic level were quantified by ARMS qPCR in a CFX96 Real-Time System (Bio-Rad) as previously reported.[26] For genotyping of FVII-iPSCs, parental fibroblasts and FVIIC-iPSC, ARMS PCR was performed by a PCR thermal cycler (Applied Biosystems Geneamp 2720) using EmeraldAmp® GT PCR Master Mix (TAKARA Bio Inc.) according to the manufacturer's instructions. Primer sequences are listed in Table 4.

4. Purification of recombinant Cas9 protein

The *Cas9* sequence was subcloned into pET28-a(+). Recombinant Cas9 protein containing a nuclear localization signal or mitochondrial localization signal with HA epitope at the N terminus or C terminus was expressed in BL21(DE3) strain, purified using Ni-NTA agarose beads (Qiagen, Düsseldorf, Germany), and dialyzed against 20 mM HEPES pH 7.5, 150 mM KCl, 1 mM DTT, and 10% glycerol. The purified Cas9 variants protein was concentrated using Ultracel 100K cellulose column (Millipore, Burlington, Massachusetts). The purity and concentration of Cas9 protein were analyzed by SDS-PAGE.

5. *in vitro* transcription for single guide RNA

Single guide RNA was in vitro transcribed by T7 RNA polymerase using MEGAshortscript T7 Kit (Thermo Fisher Scientific) according to the manufacturer's manual. Templates for sgRNA were generated by annealing and extension of two complementary oligonuceotides (Table 3). Transcribed RNA was purified by RNeasy MinElute Cleanup Kit (Qiagen) according to the manufacturer's manual.

6. Transfection

To manipulate mtDNA in patient-derived cells by RNP complex, 10^6 cells were transfected with 22.5 μg of Cas9 protein premixed with 12.5 μg of in vitro transcribed sgRNA. Cas9 protein in storage buffer (20 mM HEPES pH 7.5, 150 mM KCl, 1 mM DTT, and 10% glycerol) was mixed with sgRNA dissolved in nuclease-free water and incubated at room temperature. After 15 minutes, patient-derived cells was mixed with premixed RNP complex and pulsed twice with a voltage of 1200 for 30 ms using Neon™ Transfection System (Thermo Fisher Scientific).

For plasmid-mediated expression of mitoCas9 and sgRNA, 5 X 10^5 cells were co-transfected with 2 μg of Cas9-encoding plasmid and 2 μg of sgRNA-expressing plasmid in patient-derived cells with Lipofectamine 3000 (Thermo Fisher Scientific) according to the manufacturer's protocol. Cells were harvested and analyzed 2 days after transfection.

7. *in vitro* cleavage assay

100 ng of linearized plasmid containing target site for sgRNA was incubated for 60 min at 37 °C with 1.3 μg of Cas9 protein and 1 μg of sgRNA in 20 μg of NEB 3 buffer (1 X). Products were resolved with 0.8% agarose gel electrophoresis and visualized with EtBr staining.

8. Immunocytochemistry

Cells were fixed with 4% paraformaldehyde for 15 minutes at room temperature. After permeabilization with 0.1% Triton X-100 in PBS, cells were blocked with 2% BSA-PBS for 1 hour at room temperature and incubated overnight at 4 °C with primary antibodies in 2% BSA-PBS (Table 1). Cell were then washed, labeled with fluorescence-tagged secondary antibodies (Thermo Fisher Scientific) for 30 minutes at room temperature and mounted in DAPI mounting medium (Vector Laboratories, California, USA). Mitochondria was stained with MitoTracker™ Red CMXRos (Thermo Fisher Scientific) according to the manufacturer's protocol. Images were obtained with an Olympus IX71 microscope equipped with a DP71 digital camera (Olympus FSX100 system) or Zeiss LSM 700 confocal microscopy (ZEIZZ).

9. Live cell oxygen consumption

XF24 extracellular flux analyzers (Seahorse Biosciences, Massachusetts, USA) were used to measure oxygen consumption rates (OCR) as manufacturer's protocol. In brief, eGFP(+) and eGFP(-) neural precursor cells were seeded at a density of 10^5 cells per well of a XF24 cell culture microplate and incubated for 1 day to ensure attachment. Before assay, cells were equilibrated for 1 hour in unbuffered XF assay medium with 25 mM glucose, 1 mM sodium pyruvate, 2 mM glutamax, 1X nonessential amino acids in a non-

CO_2 incubator. Mitochondrial processes were examined through sequential injections of 0.5 μg/ml oligomycin, 1 mM carbonyl cyanide 4-(trifluoromethoxy) phenylhydrazone (FCCP) and 0.5 mM rotenone/1 mM antimycin A. Indices of mitochondrial function were calculated according to the manufacturer's instructions.

10. Differentiation into three germ layers

To test the differentiation of FVII-iPSCs *in vitro*, embryoid bodies (EBs) were formed by partial dissociation and cultured in DMEM/F12 (1:1) medium supplemented with 20% knockout serum (Invitrogen), 4.5 g/L L-glutamine, 1% NEAA, 0.1 mM 2-mercaptoethanol, and 15% FBS. 7 days after induction, EBs were attached onto Matrigel-coated culture dishes and further cultured for 14 days. Spontaneous differentiation of EBs into the three germ layer lineages was detected by immunostaining with appropriate antibodies (Table 1).

11. Karyotyping and mycoplasma testing

G-banding karyotype analysis was performed at passage 16 at GenDix, Inc. using standard protocols for GTG banding. Total 20 metaphases were analyzed at 550 band resolution. The absence of mycoplasma contamination was tested by e-Myco™ Mycoplasma PCR Detection Kit (iNtRON Biotechnology).

12. STR analysis

STR assay was performed by Cosmogenetech co, Ltd. (Korea). Briefly, the target loci were amplified using PowerPlex® 18D System Kit (Promega, Wisconsin, USA) and analyzed with ABI3130xl genetic analyzer (Applied Biosystems) using the software program GeneMapper v.5.0 (Applied Biosystems).

13. Statical analysis

Data are shown as the mean ± SEM of at least three independent experiments. Data were analyzed using the paired/unpaired, two-tailed Student's *t*-tests or analyses of variance (ANOVA) when two or more groups were involved.

Table 1. Antibodies used for immunocytochemistry

Antibody	Dilution	Company Cat #
Rabbit anti-OCT4	1:200	Santa Cruz, cat #sc-9081
Rabbit anti-SOX2	1:200	Millipore, cat # AB5603
Goat anti-NANOG	1:50	R&D systems, cat #AF1997
Mouse anti-SSEA4	1:200	Millipore, cat #MAB4304
Mouse anti-TRA-1-81	1:100	Millipore, cat #MAB4381
Mouse anti-TRA-1-60	1:100	Millipore, cat #MAB4360
Rabbit anti-NESTIN	1:1000	Millipore, cat #ABD69
Goat anti-HNF3β	1:100	Santa Cruz, cat #sc-6554
Rabbit anti-BRACHYURY	1:100	Santa Cruz, cat #sc20109
Mouse anti-HA	1:400	Santa Cruz, cat #sc-7392

Table 2. List of primers for qPCR

Target	Forward/Reverse primer (5′-3′)
OCT4 (164 bp)	CCTCACTTCACTGCACTGTA CAGGTTTTCTTTCCCTAGCT
SOX2 (80 bp)	TTCACATGTCCCAGCACTACCAGA TCACATGTGTGAGAGGGGCAGTGTGC
NANOG (154 bp)	TGAACCTCAGCTACAAACAG TGGTGGTAGGAAGAGTAAAG
TET1 (165 bp)	CTGCAGCTGTCTTGATCGAGTTAT CCTTCTTTACCGGTGTACACTACT
REX1 (145 bp)	TCACAGTCCAGCAGGTGTTTG TCTTGTCTTTGCCCGTTTCT
GAPDH (159 bp)	CAATGACCCCTTCATTGACC TTGATTTTGGAGGGATCTCG

Table 3. List of oligomers for sgRNA and ssODN

Name	Sequence
sgRNA for Exon5 top	cacc GCCTCAAGTCCATGACAGAA
sgRNA for Exon5 bottom	aaac TTCTGTCATGGACTTGAGGC
sgRNA for Exon9 top	cacc GGCATCGTCAGCTGGGGCTA
sgRNA for Exon9 bottom	aaac TAGCCCCAGCTGACGATGCC
sg3243-1 for IVT F	GAA ATT AAT ACG ACT CAC TAT AGA CAG GGT TTG TTA AGA TGG CGT TTT AGA GCT AGA AAT AGC AAG
sg3243-2 for IVT F	GAA ATT AAT ACG ACT CAC TAT AGC AGG GTT TGT TAA GAT GGC AGT TTT AGA GCT AGA AAT AGC AAG
sg3243-3 for IVT F	GAA ATT AAT ACG ACT CAC TAT AGT TTG TTA AGA TGG CAG GGC CGT TTT AGA GCT AGA AAT AGC AAG
sgRNA universal_R IVT	AAA AAA GCA CCG ACT CGG TGC CAC TTT TTC AAG TTG ATA ACG GAC TAG CCT TAT TTT AAC TTG CTA TTT CTA GCT CTA AAA C
ssODN for FVII exon 5	CCA GCC CAC TCC ACA GAT GGG GAC CAG TGT GCC TCA AGT CCA TGC CAG AAT GGG GGC TCC TGC AAG GAC CAG CTC CAG TCC TAT ATC TGC
ssODN for FVII exon 9	ACT ACC GGG GCA CGT GGT ACC TGA CGG GCA TCG TCA GCT GGG GCC AGG GCT GCG CAA CCG TGG GCC ACT TTG GGG TGT ACA CCA GGG TCT

Table 4. List of qPCR primer for mtDNA contents

Name	Sequence
3243 WT	CAG GGT TTG TTA AGA TGG CAT A
3243 MT	CAG GGT TTG TTA AGA TGG CAT G
3243 Reverse	TGG CCA TGG GTA TGT TGT TA
Actin_F	GCG CAA GTA CTC TGT GTG GA
Actin_R	CAT CGT ACT CCT GCT
12s rRNA-F	CTC ACC ACC TCT TGC TCA G
12s rRNA-B	GGC TAC ACC TTG ACC TAA CG

III. RESULTS

PART I. Specific genome editing of disease-related mutant mitochondrial DNA in patient-derived cells via CRISPR/Cas9 system

1. Generation and cellular localization of mitochondria specific Cas9 (mitoCas9)

CRISPR/Cas9 system consists of Cas9 protein and single-guide RNA (sgRNA). For CRISPR/Cas9 system to work in the mitochondria, it is necessary to translocate them to the mitochondria properly. So, I checked the localization of several Cas9 variants in the cytoplasm (Figure 1). Cas9 without localization signal was widely spread in cytosol (Figure 1B). To make a mitochondria-specific Cas9 (mitoCas9), Cas9 was conjugated with mitochondrial localization signal peptide (MLS) of human superoxide dismutase2 (SOD2)[16] to both the N-terminus and C-terminus or to one side (Figure 1A). After transfection of each plasmid into SH-SY5Y cells, it was confirmed whether each protein migrates to mitochondria or not. Cas9 with the C-terminal SOD2 MLS was unable to migrate to the mitochondria like the general Cas9 and spread widely in cytosol. On the other hands, Cas9s with N-terminal MLS effectively migrated to mitochondria (Figure 1B). Of the two versions of Cas9 with N-terminal MLS (MLS-Cas9, MLS-Cas9-MLS), I decided to proceed further experiments with Cas9 fused with N-terminal MLS.

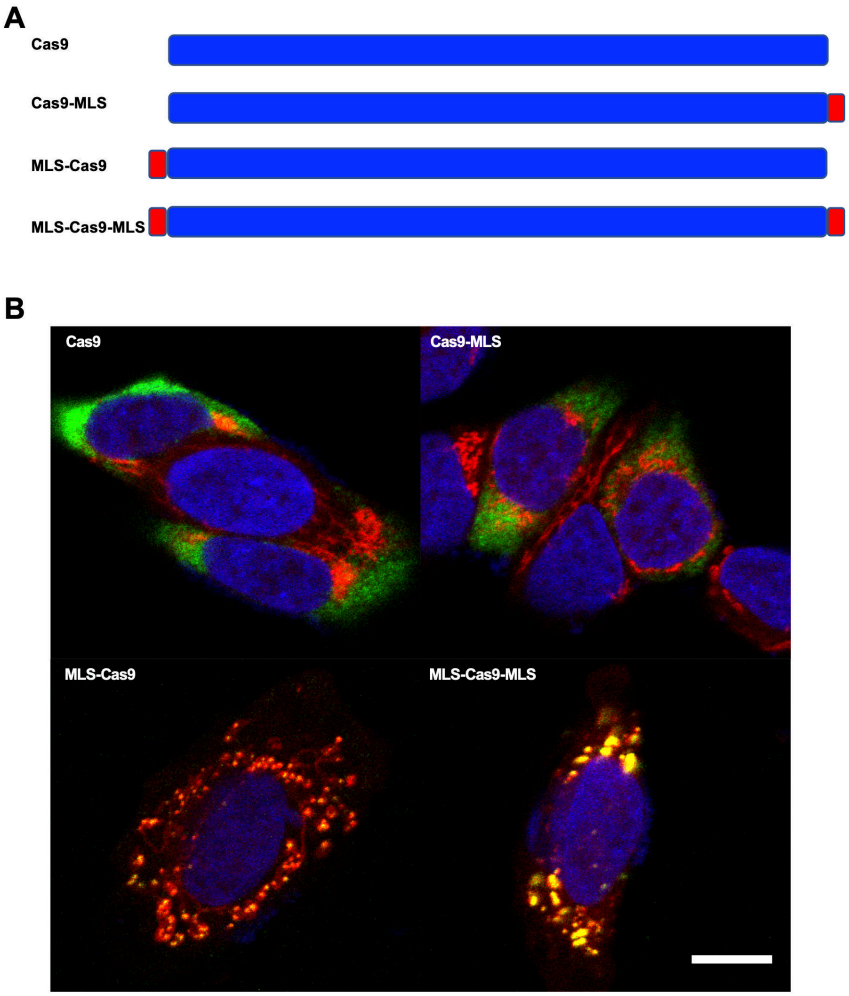

Figure 1. Localization of Cas9 variants. (A) Schematic diagram of several MLS-conjugated Cas9 variants. Blue represents Cas9 and red represents SOD2 MLS. (B) The intracellular distribution of Cas9 without or with MLS at N-terminus or C-terminus was confirmed. Cas9 without localization signal and conjugated with MLS at C-terminus were not translocate to mitochondria. Only Cas9s with N-terminal MLS were effectively moved to mitochondria. Blue channel is DAPI, green is Cas9 and red is mitochondria stained with mitotracker.

2. Cellular localization of single guide RNA (sgRNA) and effect of CRISPR/mitoCas9 delivered by plasmid

sgRNA has a more difficult problem in moving to the mitochondria from nucleous. There are several studies for import of RNA to mitochondria, but it is known that only some RNAs with special structures can migrate from the nucleus to the mitochondria.[10,27-34] To check the localization of sgRNA, I visualized sgRNA using fluorescent *in situ* hybridization (FISH). The results showed that almost sgRNA was trapped in nucleus and failed to come out of the nucleus (Figure 2A). To test the nuclease activity of CRISPR/mitoCas9 in mitochondria, I measured total copy numbers of mitochondrial genome by qPCR after transfection. LHON (3460) cell line, homoplasmic cell line containing only the mt.3460A>G mutant causing Leber hereditary optic neuroretinopathy (LHON),[35] was transfected with plasmids encoding mitoCas9 and sgRNA against mt.3460A>G mutant. 2 days after transfection, whole genomic DNA were extracted and subjected to qPCR for measuring total copy number of mtDNA. As expected, mitoCas9/sgRNA delivered by plasmid form did not change the amount of mtDNA (Figure 2B).

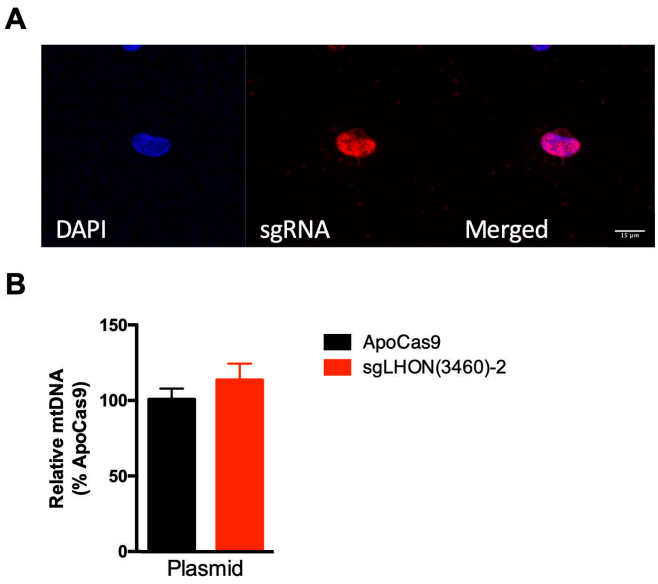

Figure 2. Localization of sgRNA and effect of CRISPR/mitoCas9 delivered by plasmid. (A) Location of sgRNA was visualized by FISH after transfection. Almost sgRNAs were trapped in nucleus. (B) mitoCas9/sgRNA delivered by plasmid did not change the amount of mtDNA in homoplasmic mutant cells.

3. Manipulation of mitochondrial DNA by mitoCas9/sgRNA ribonucleoprotein (RNP) complex

As previously mentioned, mitoCas9 translocated to the mitochondria as expected, but sgRNA was trapped in the nucleus and could not move to the mitochondria. For this reason, I thought that the expected mitochondrial genome editing was not occurred. To solve this problem, I decided to inject sgRNA into the cytoplasm using RNPs complex. Recombinant mitoCas9 protein complexed with *in vitro* transcribed sgRNA can be directly delivered to cytoplasm by electroporation. Moreover, this method enables efficient gene editing with reducing off-target effects.[36,37] A days after electroporation to LHON (3460) cells with RNP complex, the total genomic DNA was extracted from the cells and the amount of mtDNA was measured. I found that total copy number of mtDNA in LHON (3460) cells with mutant specific sgRNA were reduced compared to the control group which was electroporated only mitoCas9 protein without gRNA. To confirm whether these effects were gRNA-specific or not, I performed the same experiment on wild type cells, K562 cells, and there were no changes in total copy number of mtDNA in K562 cells. To check that this effect was caused by mitoCas9 or not, I made RNP complexes with Cas9 containing nuclear localization signal (NLS) (Cas9-NLS), and then electroporated into LHON (3460) cells. Cas9-NLS RNP complex did not change the total amount of mtDNA. Therefore, it was confirmed that the RNP complex using mitoCas9 works on mtDNA. From

these observations, I concluded that the mitoCas9 RNP complex delivered by the electroporation can be used for the mitochondria genome manipulation.

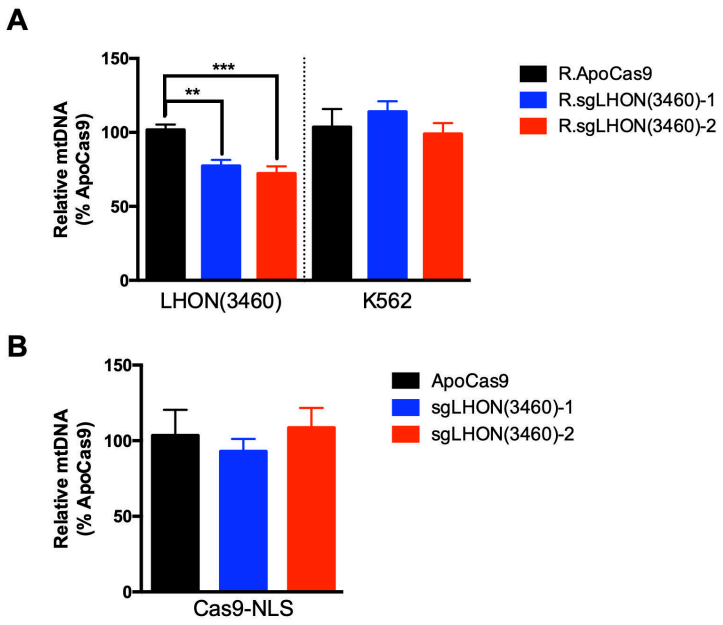

Figure 3. Mitochondrial genome was modulated by mitoCas9 RNP complex. (A) The mitoCas9/sgRNA RNP complex decreased total mutant mtDNA of LHON (3460) disease model cells, but not wild type mtDNA of K562 cells. (B) RNP complex with Cas9-NLS did not reduce total mtDNA in LHON (3460). **p<0.01, ***p<0.001 compared to negative control

4. Effect of mitoCas9/gRNA RNP complex on patient-derived heteroplasmic cell line

The previous results were obtained from homoplasmic mutant cell lines. So, it was difficult to know whether the mitoCas9 RNP complex affected to only mutant mtDNA or not. Moreover, the diseases caused by mitochondrial mutation were related with their heteroplasmy level.[12-14] To check that genotype of heteroplasmic cells could be changed by the mitoCas9 RNP complex, I performed next experiment in the heteroplasmic cell line, which was patient-derived cells carrying mt.3243A>G mutant mtDNA causing Myopathy, Encephalopathy, Lactic Acidosis, and Stroke-like episodes (MELAS). This cell line contained about 13% of wild type in total mtDNA (Figure 4B). 1 day after transfection of mitoCas9 RNP complex, changes in total amount of mtDNA and heteroplasmic level were measured by qPCR. I used three candidate sgRNAs and one sgRNA (sg3243-1) was able to reduce total contents of mtDNA by 20% (Figure 4A) In addition, I founded that the ratio of WT was also improved by sg3243-1 (Figure 4B). However, these changes seemed to be too small to improve the symptoms of the disease.

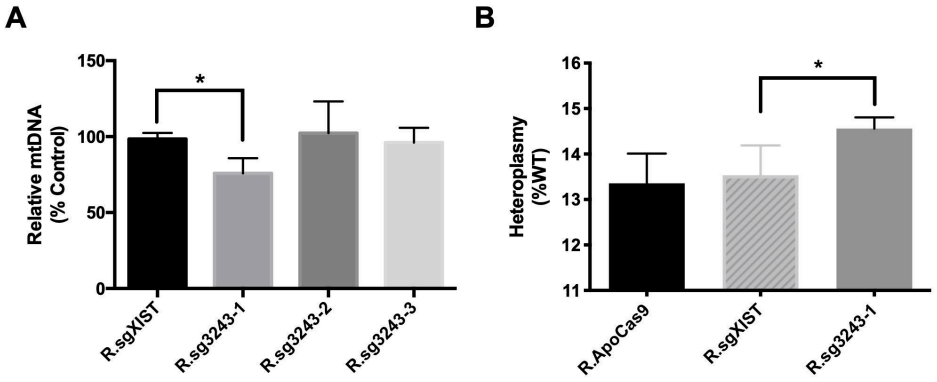

Figure 4. Effect of mitoCas9 RNP complex on heteroplasmic MELAS cell line. mitoCas9 RNP complexes with three different sgRNA against mt.3243A>G were treated to heteroplasmic MELAS cells. Among them, mitoCas9 RNP complex containing sg3243-1 was able to manipulate mtDNA. Total amounts of mtDNA were reduced (A) and heteroplasmy level was slightly increased (B) by sg3243-1. *$p<0.05$ compared to control sgRNA.

5. Cloning and characterization of mito-eGFP-Cas9

In the previous experiment, the contents of mtDNA in the heteroplasmic cells were changed by mitoCas9 RNP complex. But the change was smaller than I expected. I thought the effect of RNP complex was attenuated because these results came from the mixture of cells with and without RNP complex. So, to select the cells with RNP complex, I inserted enhanced green fluorescent protein (eGFP) into N-terminus of mitoCas9 (mito-eGFP-Cas9) (Figure 5A). To check nuclease activity of mito-eGFP-Cas9, I performed *in vitro* cleavage assay (Figure 5B). Compared to wild type Cas9, there was no difference in nuclease activity of mito-eGFP-Cas9. Next, I treated the mito-eGFP-Cas9 RNP complex to cells and checked whether it was possible to separate cells with and without mito-eGFP-Cas9 RNP complex using FACS. The cells containing mito-eGFP-Cas9 RNP complex were successfully separated by FACS (Figure 5C). Finally, I checked the intracellular distribution of mito-eGFP-Cas9 RNP complex. mito-eGFP-Cas9 RNP complex was mainly located within cytoplasm and partially translocated to mitochondria (Figure 5D).

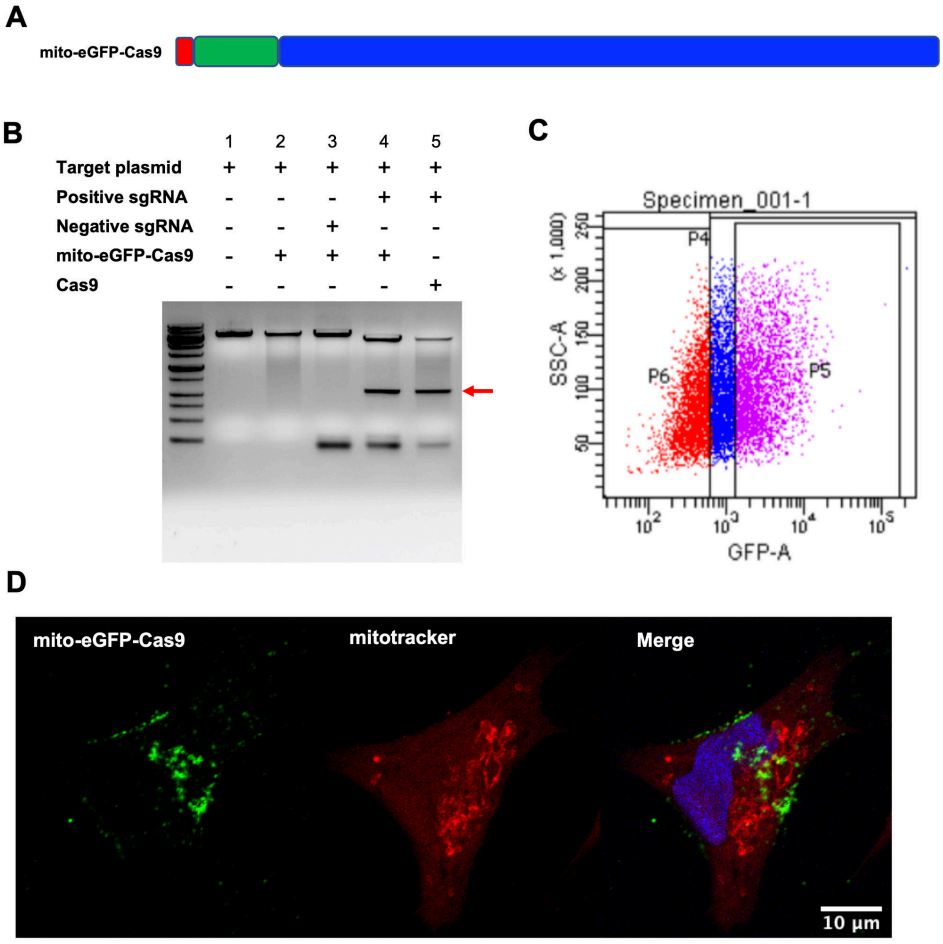

Figure 5. Cloning and characterization of mito-eGFP-Cas9. (A) Schematic diagram of mito-eGFP-Cas9. Blue represents Cas9, red SOD2 MLS, and green eGFP. (B) in vitro cleavage assay for mito-eGFP-Cas9. Red arrow indicated cleaved target plasmid. mito-eGFP-Cas9 had no problem with its nuclease activity. (C) FACS sorting after electroporation of mito-eGFP-Cas9 RNP. Cells containing mito-eGFP-Cas9 RNP complex were successfully selected and separated by FACS. (D) localization of mito-eGFP-Cas9 RNP complex. Almost of them localized in cytosol and some part translocated to mitochondria.

6. Short-term effects of mito-eGFP-Cas9/sgRNA RNP complex on patient-derived cells after enrichment by FACS sorting

To check effects of mito-eGFP-Cas9 RNP complex on mtDNA, 4 hours after transfection of mito-eGFP-Cas9 RNP complex to heteroplasmic cell line, the cells were separated into eGFP+ and eGFP- by FACS sorting. Both eGFP+ and eGFP- cells were cultured for one day and genomic DNA was extracted to measure the amount and composition of mtDNA. eGFP+ cells showed a slight increase in the heteroplasmy level (Figure 6A) and a decrease in the total amount of mtDNA (Figure 6B). However, this change has only slightly improved compared to the non-sorting group.

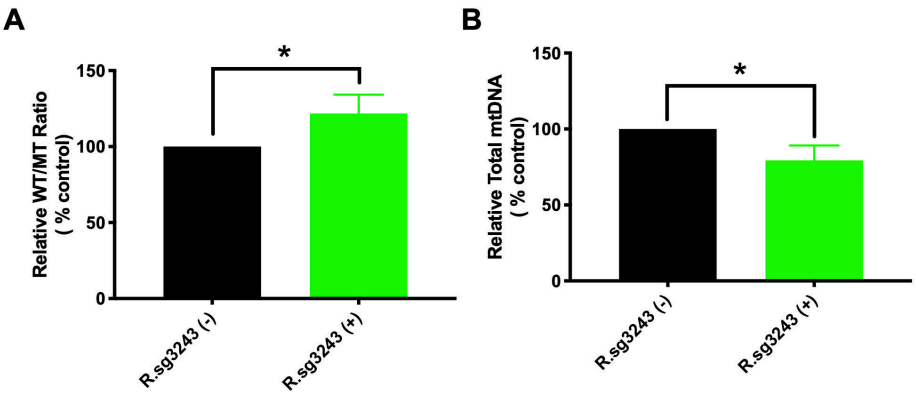

Figure 6. Short-term effects of mito-eGFP-Cas9/sgRNA RNP complex. eGFP+ cells had slightly improved heteroplasmy levels (A) and decreased total mtDNA levels (B) over eGFP- cells. *p<0.05 compared to eGFP negative control

7. Long-term effects of mito-eGFP-Cas9/sgRNA RNP complex on patient-derived cells after enrichment by FACS sorting

To confirm whether the increased heteroplasmy level is maintained and the decreased amount of mtDNA is recovered after a month, the transfected cells were processed same as described above but were cultured for a month after FACS sorting, then genomic DNA was extracted to measure the amount and composition of mtDNA. Heteroplasmy level of eGFP+ cells remained elevated state (Figure 7A) and the total amount of mtDNA that had decreased recovered to normal levels (Figure 7B). However, the heteroplasmy level has not improved any further, almost the same level as a month ago. To check if the mitochondrial function has been improved, the oxygen consumption assay was performed. There is no difference in mitochondrial function between eGFP+ cells and eGFP- cells. Although there was a slight improvement in the heteroplasmy level, it was not sufficient to bring a functional recovery of mitochondria (Figure 7C)

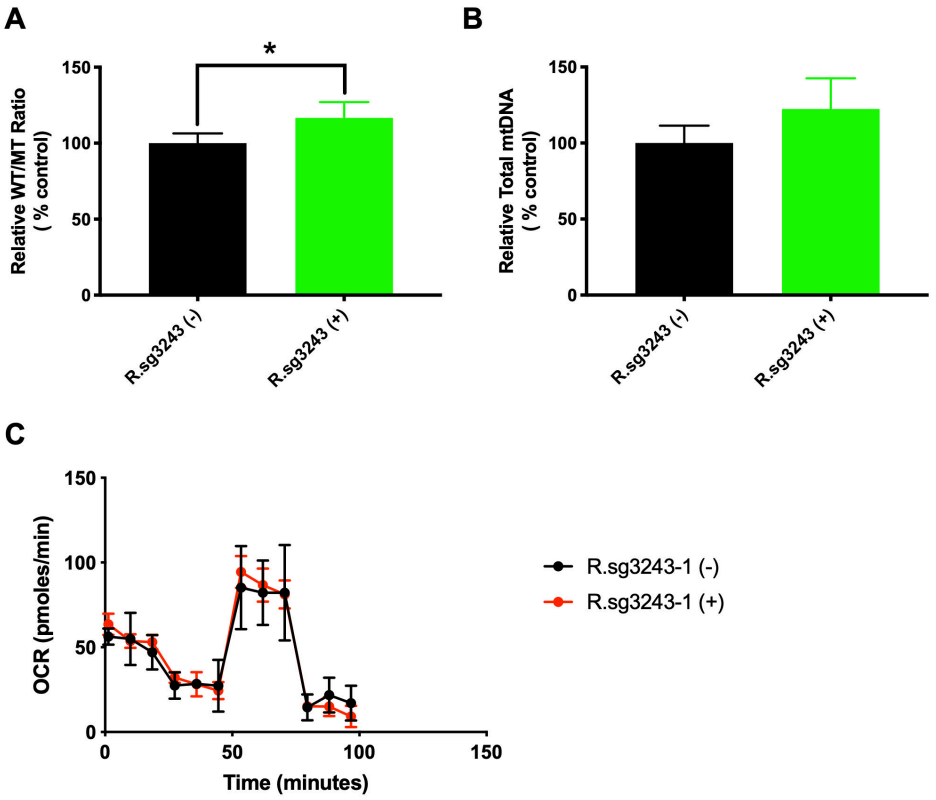

Figure 7. Long-term effects of mito-eGFP-Cas9/sgRNA RNP complex. (A) eGFP+ cells remained elevated state of heteroplasmy levels and (B) recovered total mtDNA levels. (C) There is no difference in mitochondrial function between eGFP+ cells and eGFP- cells. *p<0.05 compared to the eGFP negative control

PART II. Generation of iPSCs and gene correction from a Factor VII deficiency patient carrying FVII mutations

1. Generation of iPSCs from a Factor VII deficiency patient-derived fibroblast

First, I reprogrammed patient-derived fibroblasts into iPSCs using integration-free episomal plasmids expressing five pluripotency factors (OCT4, SOX2, KLF4, L-MYC, and Lin28) by electroporation. 10 days After the induction of iPSC, I picked several iPSC colonies with a normal human embryonic stem-cell (hESC) like morphology (Figure 8A). I checked for remaining episomal plasmids in FVII-iPSCs using PCR with episomal plasmid-specific primers for the EBNA-1 sequence. I did not detect the episomal plasmids after passage 16 or insertion into established (Figure 8B). Next, I checked the karyotypes of FVII-iPSCs line. As shown in Figure 8C, they showed a normal 46, XX karyotype after 16 passages in culture. I also confirmed that these iPSC lines were derived from parental fibroblasts and found an exact match in all the 18 STR loci analyzed, which shows that the cell line was not contaminated by any other human cell lines and genetically identical with parental fibroblasts (Figure 8D).

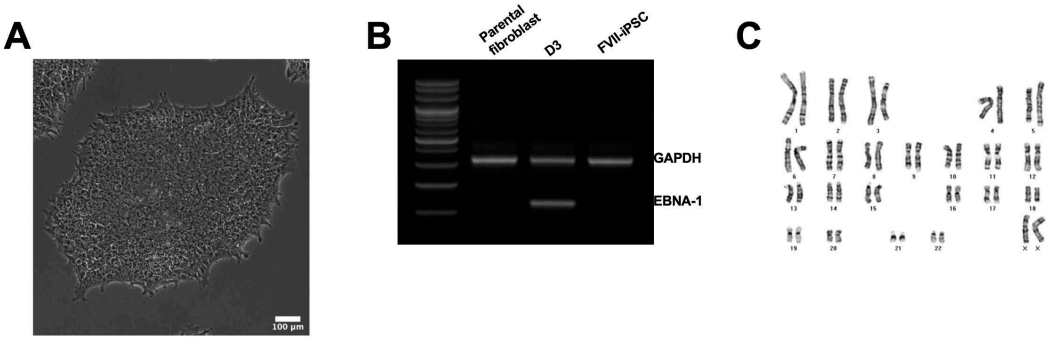

D

Match Analysis

Locus	Reference Database Profile Database : F7_ fibroblast	Sample Profile Sample Name : F7_epi7	Shared alleles #
Number of shared alleles			34
Total number of alleles in the reference database profile			34
% match			100.0%
Result interpretation			**Related**

Figure 8. Generation of FVII deficiency patient-derived iPSCs. (A) The established iPSCs were similar to ESCs. (B) PCR with episomal plasmid-specific primers for the EBNA-1 sequence. There were no episomal plasmids after passage 16. (C) FVII-iPSCs showed a normal karyotype. (D) STR assay revealed that the cell line was genetically identical with parental fibroblasts.

2. Pluripotency analysis of FVII-iPSCs

I determined whether FVII-iPSCs had pluripotency like normal hESCs. I checked the expressions of several pluripotency markers by immunostaining. These colonies highly expressed the pluripotency markers (OCT4, SOX2, and NANOG), and the surface markers (SSEA4, TRA-1- 81, and TRA-1-60) (Figure 9A). The expression level of pluripotency markers measured using quantitative-polymerase chain reactions (PCR) in FVII-iPSCs was similar to hESC H9 (Figure 9B). Pluripotency was further evaluated by differentiation of three germ layers. Using embryoid body (EB) formation assay, I demonstrated that FVII-iPSCs could be differentiated into the principal cells in three germ layers with expression of ectodermal marker Nestin, endodermal marker HNF3b, and mesodermal marker Brachyury (Figure 9C).

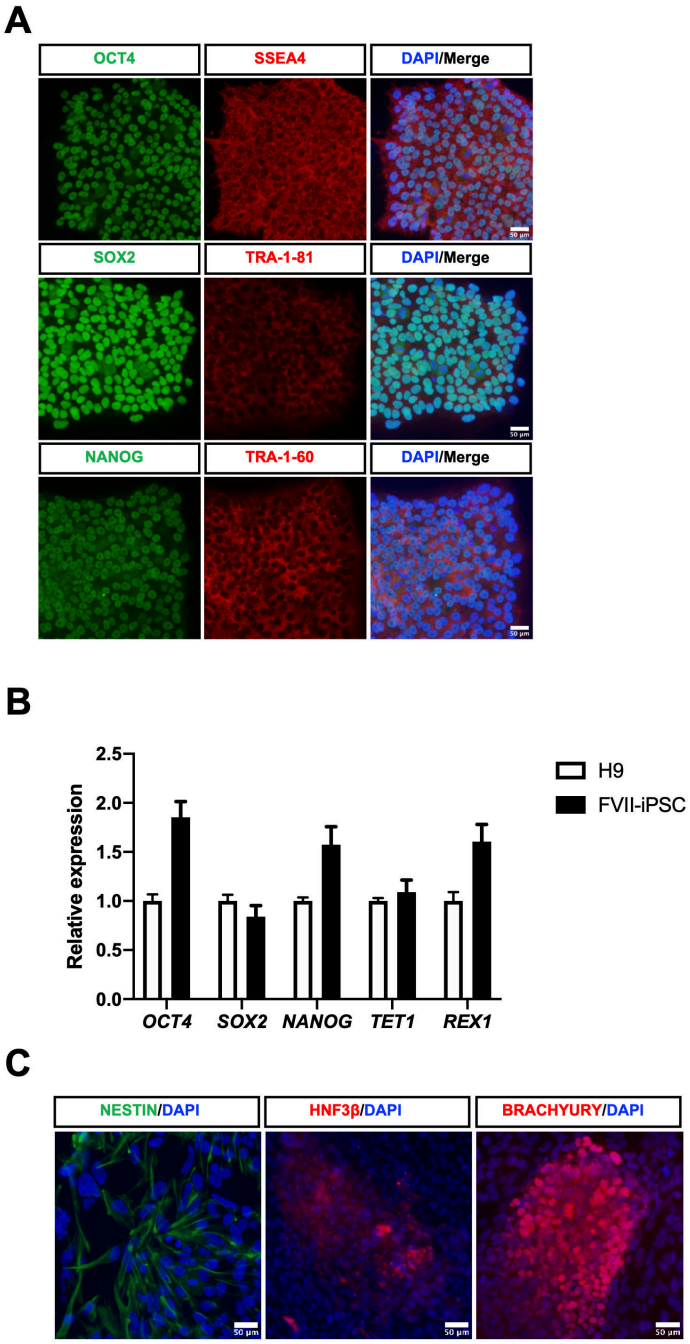

Figure 9. Pluripotency analysis of FVII-iPSCs. (A) FVII-iPSCs highly expressed the pluripotency markers (OCT4, SOX2, and NANOG), and the surface markers (SSEA4, TRA-1- 81, and TRA-1-60). (B) qPCR analysis for expression of pluripotency makers. The expression level of pluripotency marker in FVII-iPSCs was similar to normal hESC H9. (C) FVII-iPSCs could be differentiated into the principal cells in three germ layers.

3. Sequencing analysis of FVII-iPSCs and designation of sgRNA

To identify mutations in FVII-iPSCs, I checked whole sequences of exons in *FVII* loci by Sanger sequencing and identified heterozygous compound mutations. The first mutation is a well-known mutant located in exon 5 of Factor VII (c.345C>A; p.C115X), and the other is novel and located in exon 9 (c.1276C>T; p.Q426X) (Figure 10A, B). Both SNPs caused nonsense mutations. According to position of SNP, I choose specific sgRNAs against each SNP (Figure 10C). The designation of sgRNA is restricted by the protospacer adjacent motif (PAM) sequence and position of SNP. To choice best sgRNA, I searched PAM most nearby SNP and the sgRNA with the highest score was selected in the GPP sgRNA Designer.[38]

A

Exon 5 (c.345C>A;p.C115X)

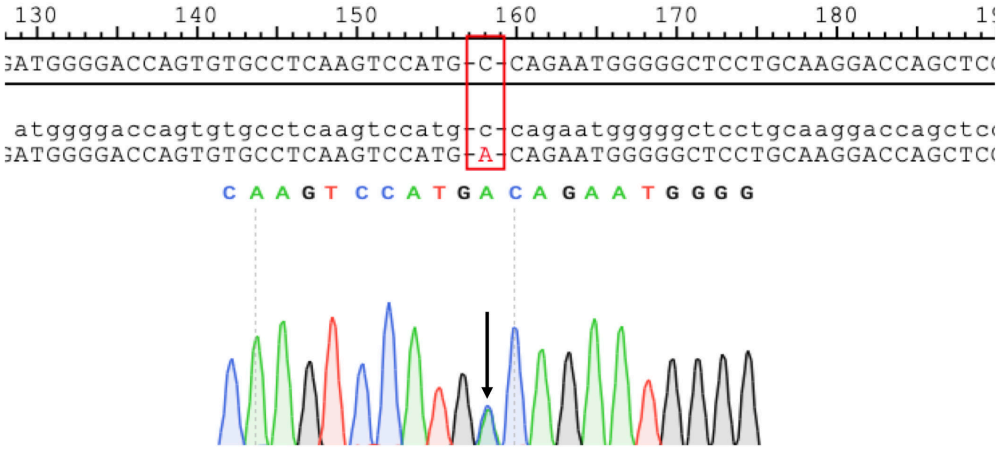

B

Exon 9 (c.1276C>T;p.Q426X)

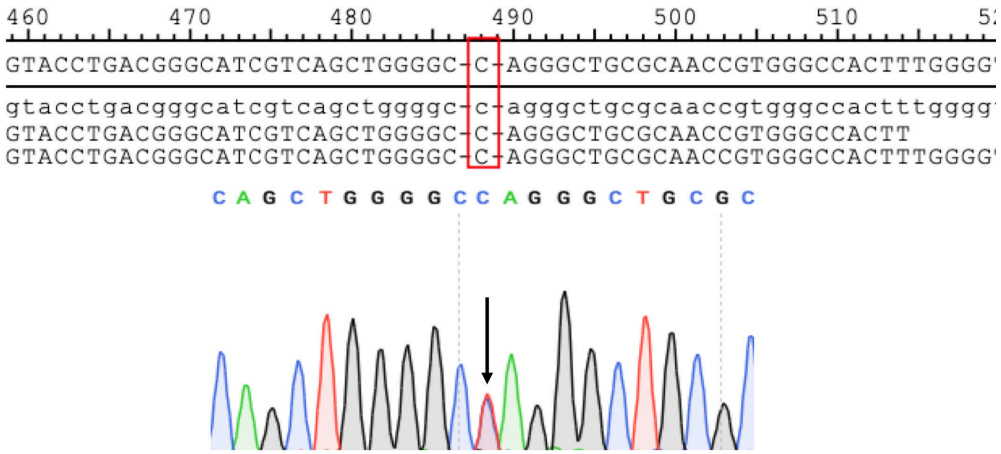

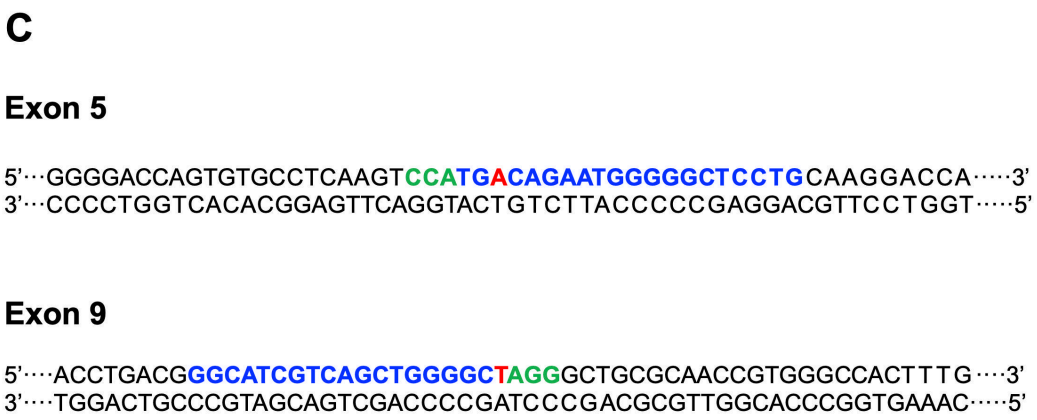

Figure 10. Mutation analysis of *FVII* locus in a FVII-iPSCs and designation of sgRNA and donor template. (A, B) Sanger sequencing for *FVII* exon regions revealed that there are compound heterozygous mutations in exon 5 (A) and exon 9 (B). The top panel is the sequencing result, and the bottom is the chromatography result. It can be confirmed that all SNPs present in each exon are heterozygote. (C) The sgRNA for each SNP was designed. The red sequences represented SNP. PAM sequences were shown in green and protospacer sequences in blue. ssODNs were prepared using the indicated whole sequence, and among them, SNP was replaced with a wild type.

4. CRISPR/Cas9 and ssODN-mediated gene corrections in FVII-iPSCs

To correct mutations in *FVII* loci, I used CRISPR/Cas9 system and ssODN as donor template. For ssODN, a wild type sequence corresponding to a total of 90 bp was selected from 45 bp upstream to 5'- and downstream to 3'-end based on the mutation position. The ssODN strategy is suitable for editing of SNP and scarless gene editing, but the lack of selectable markers within the donor makes a difficult to identify precisely edited clones. Therefore, I performed transient puromycin selection.[39](Figure 11A) Since there are two mutations in FVII-iPSCs and it is very difficult to correct them simultaneously, I attempted to correct one mutation first (c.345C>A) and then corrected the other mutations (c.1276C>T) in the corrected cells. Correction for the c.345 mutation was performed first. After selection over 2 weeks, I pick at least 10 survived colonies, and PCR was performed using primers specific for c.345C>A mutant to select the colonies whose mutations were corrected. After that, it was confirmed that the mutation was corrected through sanger sequencing. Genetic correction for c.1276C>T was again performed using the corrected colony by same way. After then, I was able to get colonies with both mutations corrected (FVIIC-iPSC) (Figure 11 B, C).

A

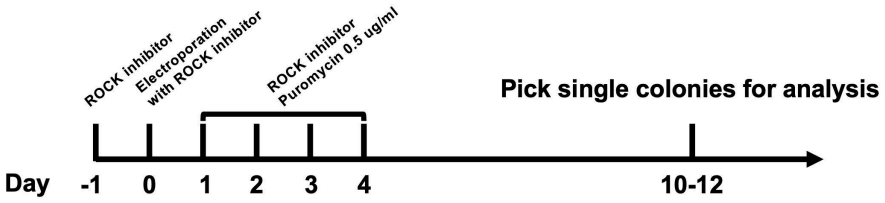

B

Exon 5 (c.345C>A;p.C115X)

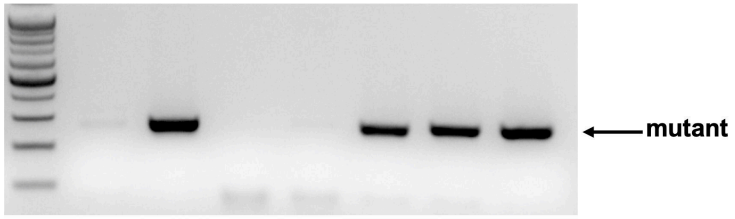

Exon 5 (c.345C>A;p.C115X)

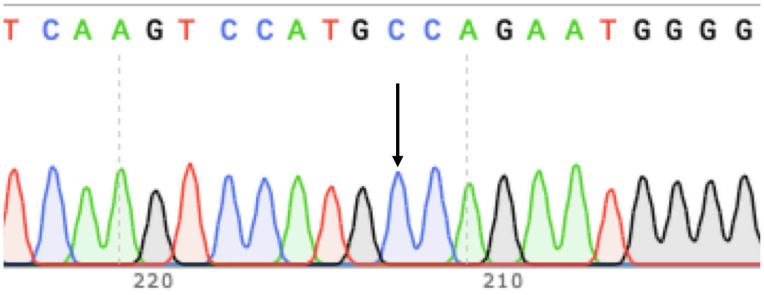

C

Exon 9 (c.1276C>T;p.Q426X)

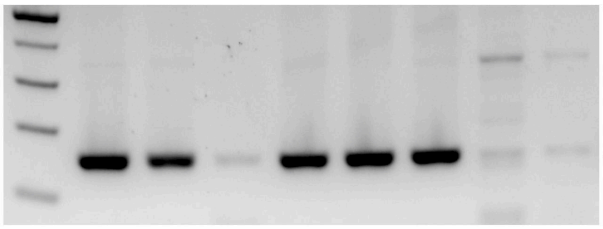

Exon 9 (c.1276C>T;p.Q426X)

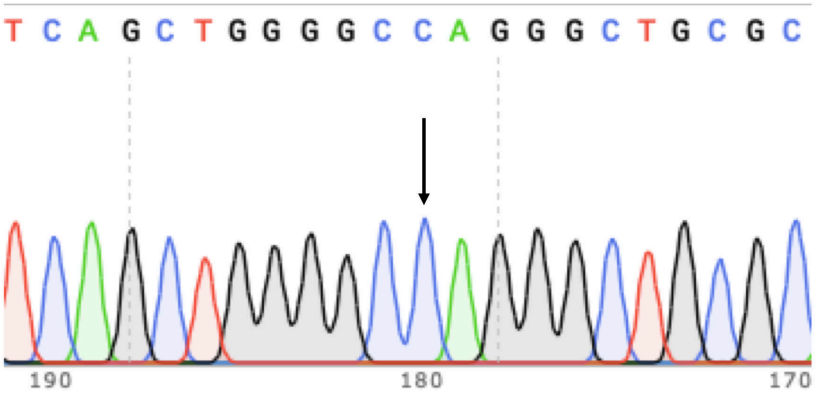

Figure 11. Gene correction in FVII-iPSCs using CRISPR/Cas9 system and ssODN donor template. (A) Experimental scheme for genetic correction. A day before electroporation, ROCK inhibitor was treated. After electroporation, the FVII-iPSCs were cultured with puromycin for 3 days, and then puromycin was withdrew. The FVII-iPSCs were culture in normal media for 7-9 days after withdrawal. Remaining colonies were isolated and analyzed. (B, C) correction result in exon 5 (B) and exon 9 (C). Upper panel showed primary PCR screening result with SNP-specific primers. After gene correction, there are no SNP-specific amplification. Lower panel was Sanger sequencing result to confirm whether SNP was corrected or not. SNPs were successfully replaced to wild type sequences.

5. Restoration of FVII activity in gene-corrected iPSC-derived hepatocyte like cells

Finally, I performed the FVII activity assay to check whether FVII function of the corrected cells was restored. FVII is known to be mainly secreted by hepatocytes.[40,41] Gene-corrected iPSCs were differentiated to hepatocyte-like cells (HLCs) as previous report.[42] In the differentiated HLCs, the expression of alpha-fetoprotein (AFP), a hepatocyte precursor marker, and albumin (ALB), a hepatocyte marker, were significantly increased at the mRNA level compared to iPSCs (Figure 12A). FVII-iPSCs, FVIIC-iPSCs, and H9 were differentiated according to the established differentiation methods, and FVII activity assays were performed. FVII activity, which was decreased in patient-derived cells, was increased, which was similar to that of the wild type H9 (Figure 12B).

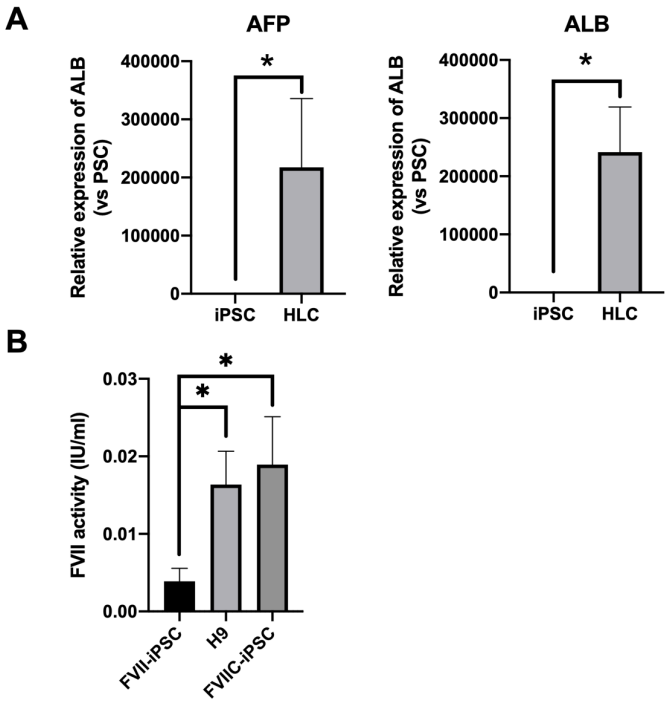

Figure 12. Differentiation of iPSCs into HLCs and restoration of FVII activity. (A) qPCR analysis for expression of hepatocyte makers. The expression level of hepatocyte marker in HLCs was increased compared to iPSCs. (B) FVII activity in FVII-iPSC, FVIIC-iPSC and H9 derived HLC. Decreased FVII activity in FVII-iPSC derived HLCs was restored in FVIIC-iPSC derived HLCs. *$p<0.05$ compared to the control

IV. DISCUSSION

This study aimed to use a CRISPR/Cas9 system to correct mutations in patient-derived cells carrying disease-related SNPs. Two types of disease-related SNPs were selected; one occurs in the mitochondrial genome and the other occurs in coagulation factor FVII. Because each mutation has different characteristics, the approach for each gene correction was quite different. In this study, gene editing methods have been established that are suitable for each disease.

Part I. Specific genome editing of disease-related mutant mitochondrial DNA in patient-derived cells via CRISPR/Cas9 system

The CRISPR/Cas9 system is an emerging technique that has been widely applied for genome modifications in human cells. However, there is still debate about whether or not this technique can be utilized for mitochondrial DNA editing.[18-20,43] The translocation of DNA or RNA from the cytosol into mitochondria is difficult because only RNA or DNA with a specific structure can enter the mitochondria.[27,29,30,32,44] Because of this, there is some disagreement about whether or not sgRNA could migrate into mitochondria.[19,20,43] This study determined that sgRNA expressed by plasmid in the cell was trapped in the nucleus and could not translocate into mitochondria. Therefore, the CRISPR/Cas9 system did not

work for the plasmid expression method (Figure 1, 2). Next, an experiment was conducted in which a CRISPR/Cas9 RNP complex was used to inject Cas9 and sgRNA directly into the cytoplasm. For this RNP method, the amount of mtDNA decreased in the mutant cell line and the ratio of wild type to mutant mtDNA was higher (Figure 3, 4, 6, 7). However, its efficiency was lower than other previously reported protein-based engineered nucleases such as ZFN and TALEN.[15-17] The RPN method did not lead to the functional recovery of patient-derived cells due to its low editing efficiency (Figure 7).

The RNP complex method has a couple of major limitations compared to the plasmid delivery method. The low effectiveness of the mitoCas9 RNP complex seemed to be due to the low translocation efficiency of the mitoCas9 RNP complex to the mitochondria and the short lifespan of the RNP complex. It was confirmed that most of the mitoCas9 RNP complex delivered into the cell was present in cytosol, and only a small amount of mitoCas9 RNP complex migrated to a limited number of mitochondria (Figure 5D). By contrast, protein-based engineered nucleases can migrate to mitochondria and act on almost every mitochondrion.[15-17] The short half-life of the RNP complex seemed to be another limitation of mitochondrial genome editing. Generally, RNP complexes disappear 24 hours after transfection, but the expression of nuclease delivered by plasmid continues for up to 72 hours after transfection,[36] which is enough time to correct a large number of mtDNA.

In the future, mitochondrial genome editing by CRISPR/Cas9 could be improved by finding a way for sgRNA to migrate efficiently into mitochondria[19] and increasing the intracellular lifespan of the RNP complex.[45]

Part II. Generation of iPSCs and gene correction from a Factor VII deficiency patient carrying FVII mutations

FVII deficiency is caused by mutations in the genes of coagulation Factor VII. The mutations that occur in *FVII* loci exist in various forms and are primarily SNPs in exon. Symptoms of FVII deficiency, depending on the SNPs, also occur to different degrees.[46,47] Especially among FVII patients, there are many cases of compound heterozygous mutations, which lead to diverse symptoms of the disease.[47] The genotype of the patient-derived cells used in this study consisted of compound heterozygotes with two mutations, one that is well-known and one novel mutation (Figure 10).

Gene correction of SNPs requires only small parts of the mutant sequence to be replaced with wild type. This enables the use of ssODNs as a donor template rather than complex donor plasmid DNA. ssODNs also have the advantage of being able to correct sequences more efficiently than large donor plasmid DNA, and they are less likely to involve unnecessary sequences in the correction site.[48,49] However, when using ssODN as the donor template, it is difficult to select gene-corrected cells because of the absence of a

selection marker that is usually included in the donor plasmid DNA. Moreover, the patient-derived cells used in this study have two mutations in different locations of the *FVII* loci (Figure 10). It is difficult to correct these two SNPs simultaneously, so it is necessary to correct each mutation sequentially and quickly. Therefore, an efficient selection method is needed to reduce the duration of the sequential correction. This problem was solved by using the Cas9 selection marker in the plasmid DNA,[39] which was able to effectively select gene-corrected cells within a short period compared to the common method of including selective antibiotics in the donor plasmid DNA (Figure 11). After gene correction, the FVIIC-iPSCs were differentiated to HLCs. The FVII activity of FVIIC-iPSC-derived HLCs recovered to a level similar to the wild type control (Figure 12). This technique could provide a basis for cell therapy for patients with FVII deficiency.

It is difficult to correlate phenotypes (symptoms of disease) and genotypes (mutations) of FVII deficiency because of the wide range of symptoms and mutations.[22] The correction method described in this study will enable gene correction and the establishment of a disease model for various mutations, which will also help clarify the correlation between mutations and disease symptoms. In addition, the established disease model can be utilized in the development of new drugs for FVII deficiency.

V. CONCLUSION

CRISPR/Cas9 is a novel technology in the rapidly developing field of gene correction. In this study, CRISPR/Cas9 was used to edit genes in SNP-related diseases.

The CRISPR/Cas9 RNP complex provides a new approach to mitochondria gene editing. In this study, an efficient gene correction method for multiple SNPs was established for FVII-deficient patient-derived cells. The results suggest that the CRISPR/Cas9 system could potentially be applied in gene therapy and cell therapy of various SNP-related diseases.

REFERENCE

1 Park C-Y, Sung JJ, Kim D-W. Genome Editing of Structural Variations: Modeling and Gene Correction. *Trends Biotechnol* 2016; 34: 548–61.

2 Doudna JA, Charpentier E. Genome editing. The new frontier of genome engineering with CRISPR-Cas9. *Science* 2014; 346: 1258096.

3 Kim HH, Kim J-S. A guide to genome engineering with programmable nucleases. *Nat Rev Genet* 2014; 15: 321–34.

4 Landrum MJ, Lee JM, Riley GR, Jang W, Rubinstein WS, Church DM, *et al.* ClinVar: public archive of relationships among sequence variation and human phenotype. *Nucleic Acids Res* 2014; 42: D980–5.

5 Landrum MJ, Lee JM, Benson M, Brown G, Chao C, Chitipiralla S, *et al.* ClinVar: public archive of interpretations of clinically relevant variants. *Nucleic Acids Res* 2016; 44: D862–8.

6 Rees HA, Liu DR. Base editing: precision chemistry on the genome and transcriptome of living cells. *Nat Rev Genet* 2018; published online Oct 15. DOI:10.1038/s41576-018-0059-1.

7 Schon EA, DiMauro S, Hirano M. Human mitochondrial DNA: roles of inherited and somatic mutations. *Nat Rev Genet* 2012; 13: 878–90.

8 Taylor RW, Turnbull DM. Mitochondrial DNA mutations in human disease. *Nat Rev Genet* 2005; 6: 389–402.

9 Cavelier L, Johannisson A, Gyllensten U. Analysis of mtDNA copy number and composition of single mitochondrial particles using flow cytometry and PCR. *Exp Cell Res* 2000; 259: 79–85.

10 Satoh M, Kuroiwa T. Organization of multiple nucleoids and DNA molecules in mitochondria of a human cell. *Exp Cell Res* 1991; 196: 137–40.

11 Poe BG, Navratil M, Arriaga EA. Absolute quantitation of a heteroplasmic mitochondrial DNA deletion using a multiplex three-primer real-time PCR assay. *Analytical Biochemistry* 2007; 362: 193–200.

12 Bentlage HA, Attardi G. Relationship of genotype to phenotype in fibroblast-derived transmitochondrial cell lines carrying the 3243 mutation associated with the MELAS encephalomyopathy: shift towards mutant genotype and role of mtDNA copy number. *Hum Mol Genet* 1996; 5: 197–205.

13 Porteous WK, James AM, Sheard PW, Porteous CM, Packer MA, Hyslop SJ, *et al.* Bioenergetic consequences of accumulating the common 4977-bp mitochondrial DNA deletion. *Eur J Biochem* 1998; 257: 192–201.

14 Wallace DC. Mitochondrial diseases in man and mouse. *Science* 1999; 283: 1482–8.

15 Bacman SR, Williams SL, Pinto M, Peralta S, Moraes CT. Specific elimination of mutant mitochondrial genomes in patient-derived cells by mitoTALENs. *Nat Med* 2013; 19: 1111–3.

16 Hashimoto M, Bacman SR, Peralta S, Falk MJ, Chomyn A, Chan DC, *et al.* MitoTALEN: A General Approach to Reduce Mutant mtDNA Loads and Restore Oxidative Phosphorylation Function in Mitochondrial Diseases. *Mol Ther* 2015; 23: 1592–9.

17 Gammage PA, Rorbach J, Vincent AI, Rebar EJ, Minczuk M. Mitochondrially targeted ZFNs for selective degradation of pathogenic mitochondrial genomes bearing large-scale deletions or point mutations. *EMBO Mol Med* 2014; 6: 458–66.

18 Jo A, Ham S, Lee GH, Lee Y-I, Kim S, Lee Y-S, *et al.* Efficient Mitochondrial Genome Editing by CRISPR/Cas9. *Biomed Res Int* 2015; 2015: 305716–10.

19 Loutre R, Heckel A-M, Smirnova A, Entelis N, Tarassov I. Can Mitochondrial DNA be CRISPRized: Pro and Contra. *IUBMB Life* 2018; 70: 1233–9.

20 Gammage PA, Moraes CT, Minczuk M. Mitochondrial Genome Engineering: The Revolution May Not Be CRISPR-Ized. *Trends Genet* 2017; 34: 101–10.

21 Perry DJ. Factor VII Deficiency. *Br J Haematol* 2002; 118: 689–700.

22 Lapecorella M, MARIANI G, International Registry on Congenital Factor VII

Deficiency. Factor VII deficiency: defining the clinical picture and optimizing therapeutic options. *Haemophilia* 2008; 14: 1170–5.

23 Kwon M-J, Yoo K-Y, Lee K-O, Kim SH, Kim H-J. Recurrent mutations and genotype-phenotype correlations in hereditary factor VII deficiency in Korea. *Blood Coagul Fibrinolysis* 2011; 22: 102–5.

24 Okita K, Matsumura Y, Sato Y, Okada A, Morizane A, Okamoto S, *et al.* A more efficient method to generate integration-free human iPS cells. *Nat Methods* 2011; 8: 409–12.

25 Jang J, Kang H-C, Kim H-S, Kim JY, Huh YJ, Kim D-S, *et al.* Induced pluripotent stem cell models from X-linked adrenoleukodystrophy patients. *Ann Neurol* 2011; 70: 402–9.

26 Bai R-K, Wong L-JC. Detection and quantification of heteroplasmic mutant mitochondrial DNA by real-time amplification refractory mutation system quantitative PCR analysis: a single-step approach. *Clin Chem* 2004; 50: 996–1001.

27 Comte C, Tonin Y, Heckel-Mager A-M, Boucheham A, Smirnov A, Auré K, *et al.* Mitochondrial targeting of recombinant RNAs modulates the level of a heteroplasmic mutation in human mitochondrial DNA associated with Kearns Sayre Syndrome. *Nucleic Acids Res* 2013; 41: 418–33.

28 Gowher A, Smirnov A, Tarassov I, Entelis N. Induced tRNA import into human

mitochondria: implication of a host aminoacyl-tRNA-synthetase. *PLoS ONE* 2013; 8: e66228.

29 Wang G, Shimada E, Koehler CM, Teitell MA. PNPASE and RNA trafficking into mitochondria. *Biochim Biophys Acta* 2012; 1819: 998–1007.

30 Schneider A. Mitochondrial tRNA import and its consequences for mitochondrial translation. *Annu Rev Biochem* 2011; 80: 1033–53.

31 Kolesnikova O, Kazakova H, Comte C, Steinberg S, Kamenski P, Martin RP, *et al.* Selection of RNA aptamers imported into yeast and human mitochondria. *RNA* 2010; 16: 926–41.

32 Smirnov A, Tarassov I, Mager-Heckel A-M, Letzelter M, Martin RP, Krasheninnikov IA, *et al.* Two distinct structural elements of 5S rRNA are needed for its import into human mitochondria. *RNA* 2008; 14: 749–59.

33 Kolesnikova OA, Entelis NS, Jacquin-Becker C, Goltzene F, Chrzanowska-Lightowlers ZM, Lightowlers RN, *et al.* Nuclear DNA-encoded tRNAs targeted into mitochondria can rescue a mitochondrial DNA mutation associated with the MERRF syndrome in cultured human cells. *Hum Mol Genet* 2004; 13: 2519–34.

34 Entelis NS, Kolesnikova OA, Dogan S, Martin RP, Tarassov I. 5 S rRNA and tRNA import into human mitochondria. Comparison of in vitro requirements. *J Biol Chem* 2001; 276: 45642–53.

35 Brown MD, Voljavec AS, Lott MT, MacDonald I, Wallace DC. Leber's hereditary optic neuropathy: a model for mitochondrial neurodegenerative diseases. *FASEB J* 1992; 6: 2791–9.

36 Kim S, Kim D, Cho SW, Kim J, Kim J-S. Highly efficient RNA-guided genome editing in human cells via delivery of purified Cas9 ribonucleoproteins. *Genome Research* 2014; 24: 1012–9.

37 Cho SW, Kim S, Kim Y, Kweon J, Kim HS, Bae S, *et al.* Analysis of off-target effects of CRISPR/Cas-derived RNA-guided endonucleases and nickases. *Genome Research* 2014; 24: 132–41.

38 Doench JG, Fusi N, Sullender M, Hegde M, Vaimberg EW, Donovan KF, *et al.* Optimized sgRNA design to maximize activity and minimize off-target effects of CRISPR-Cas9. *Nat Biotechnol* 2016; 34: 184–91.

39 Steyer B, Bu Q, Cory E, Jiang K, Duong S, Sinha D, *et al.* Scarless Genome Editing of Human Pluripotent Stem Cells via Transient Puromycin Selection. *Stem Cell Reports* 2018; 10: 642–54.

40 Arbini AA, Pollak ES, Bayleran JK, High KA, Bauer KA. Severe factor VII deficiency due to a mutation disrupting a hepatocyte nuclear factor 4 binding site in the factor VII promoter. *Blood* 1997; 89: 176–82.

41 Barbon E, Pignani S, Branchini A, Bernardi F, Pinotti M, Bovolenta M. An

engineered tale-transcription factor rescues transcription of factor VII impaired by promoter mutations and enhances its endogenous expression in hepatocytes. *Sci Rep* 2016; 6: 28304.

42 Viiri LE, Rantapero T, Kiamehr M, Alexanova A, Oittinen M, Viiri K, *et al.* Extensive reprogramming of the nascent transcriptome during iPSC to hepatocyte differentiation. *Sci Rep* 2019; 9: 3562–12.

43 Bian W-P, Chen Y, Luo J, Wang C, Xie S, Pei D. A knock-in strategy for editing human and zebrafish mitochondrial DNA using mito-CRISPR/Cas9 system. *ACS Synth Biol* 2019; published online April 8. DOI:10.1021/acssynbio.8b00411.

44 Lakunina VA, Baleva MV, Levitskii SA, Chicherin IV, Krasheninnikov IA, Samoylova EO, *et al.* RNA import into mitochondria and its use in gene therapy. *Moscow Univ BiolSci Bull* 2015; 70: 132–5.

45 Hendel A, Bak RO, Clark JT, Kennedy AB, Ryan DE, Roy S, *et al.* Chemically modified guide RNAs enhance CRISPR-Cas genome editing in human primary cells. *Nat Biotechnol* 2015; 33: 985–9.

46 Mariani G, Bernardi F. Factor VII Deficiency. *Semin Thromb Hemost* 2009; 35: 400–6.

47 Herrmann FH, Wulff K, Auerswald G, Schulman S, Astermark J, Batorova A, *et al.* Factor VII deficiency: clinical manifestation of 717 subjects from Europe and Latin

America with mutations in the factor 7 gene. *Haemophilia* 2009; 15: 267–80.

48 Dewari PS, Southgate B, Mccarten K, Monogarov G, O'Duibhir E, Quinn N, *et al.* An efficient and scalable pipeline for epitope tagging in mammalian stem cells using Cas9 ribonucleoprotein. *Elife* 2018; 7: e35069.

49 Paquet D, Kwart D, Chen A, Sproul A, Jacob S, Teo S, *et al.* Efficient introduction of specific homozygous and heterozygous mutations using CRISPR/Cas9. *Nature* 2016; 533: 125–9.

ABSTRACT (IN KOREA)

CRISPR/Cas9 system을 이용한 환자 유래 세포에서 두 가지 단일염기다형성에 대한 유전자 교정

< 지도교수 김 동 욱 >

연세대학교 대학원 의과학과

김 도 훈

유전자 가위인 zinc finger nuclease (ZFN), transcription activator-like effector nuclease (TALEN), 그리고 type II clustered regularly interspaced short palindromic repeats (CRISPR)/CRIPSR-associated protein 9 (Cas9) 을 이용한 표적 특이적인 유전자 교정은 인간의 유전 질환을 치료할 수 있는 좋은 방법으로 여겨지고 있다. 이 중에서 CRISPR/Cas9 은 guide RNA (gRNA) 를 이용한 표적 특이성을 쉽게 변형할 수 있어 다양한 돌연변이에 대응하기 좋다. 인간의 질환과 관련되어 있는 여러 돌연변이 중에서 58% 가 single nucleotide polymorphisms

(SNPs) 에 의해 유발된다. 특히 미토콘드리아 유전체 돌연변이 관련 질환과 FVII 응고인자 부족 혈액응고 장애의 경우 관련한 돌연변이 대부분이 SNPs 로 알려져 있다. 따라서 CRISPR/Cas9 을 활용하여 다양한 SNPs 에 의해 유발되는 질환을 치료할 수 있는 시스템을 마련할 필요가 있다. 본 연구에서는 미토콘드리아 유전체 교정을 위해 몇 가지 방법을 시도하였다. 미토콘드리아 유전체 교정의 경우, 유전자 교정에서 일반적으로 많이 사용하는 플라스미드 전달 방식으로 유전자 가위를 전달하였을 때 gRNA 가 제대로 미토콘드리아로 이동하지 못하고 이로 인해 CRISPR/Cas9 시스템이 제대로 작동하지 않음을 확인하였다. 이를 해결하기 위해 Cas9 과 gRNA 를 직접 세포 내에 넣어 주는 ribonucleoprotein (RNP) 복합체 방식을 이용한 결과 일부 지표에서 미토콘드리아의 유전형이 호전되는 결과를 확인하였다. 하지만 RNP 복합체를 이용한 미토콘드리아 교정은 그 효율이 낮아 기능적 회복에 까지는 이르지 못하였다. 그러나 이러한 접근 방식을 통해 미토콘드리아 유전체 교정에 대한 가능성을 제시하였다는 점에서 의미가 있다. 다음으로 제 7 혈액응고 인자 (FVII) 결핍증의 유전자 교정을 위해 제 7 혈액응고인자에 이형 복합 돌연 변이를 가진 환자 유래 세포로부터 유도만능줄기세포를 제작하였다. 2 개의 서로 다른 SNP 을 CRISPR/Cas9 시스템과 single-stranded oligodeoxynucleotides (ssODNs) 을 이용하여

교정을 하였고, 비교적 짧은 시간 내에 스크리닝하는 방법으로 두개의 돌연변이를 효과적으로 순차 교정하여 정상 세포로 되돌릴 수 있었다. 교정된 세포를 hepatocyte-like cells (HLCs) 로 분화한 후 FVII 활성도가 정상 세포와 유사한 수준으로 회복된 것을 확인할 수 있었다. 본 연구를 통해 CRISPR/Cas9 을 이용한 다양한 형태의 SNPs 교정에 대한 가능성을 제시하였다.

핵심되는 말: 유전자 교정, clustered regularly interspaced short palindromic repeats (CRISPR)/CRIPSR-associated protein 9 (Cas9), 미토콘드리아, 유도만능줄기세포, 제 7 혈액응고인자 결핍증

PUBLICATION LIST

1 **Kim D-H**, Park C-Y, Cho S-R, Kim D-W. Generation of a human induced pluripotent stem cell line, YCMi002-A, from a Factor VII deficiency patient carrying F7 mutations. *Stem Cell Res* 2020; 49, 102026.

2 **Kim D-H**, Shin SW, Baik J-H. Role of third intracellular loop of the melanocortin 4 receptor in the regulation of constitutive activity. *Biochem Biophys Res Commun* 2008; 365: 439–45.